Kinetic Enhancement of Hydrogen Cycling in $NaAlH_4$ by Melt Infusion into Nanoporous Carbon Aerogel

Robert D. Stephens,[a] *Adam F. Gross,*[b] *Sky L. Van Atta*[b] *John J. Vajo,*[b] *and Frederick E. Pinkerton*[c,]*

[a]Chemical and Environmental Sciences Laboratory, General Motors Research and Development Center, Warren, MI 48090-9055, USA

[b]HRL Laboratories, LLC, 3011 Malibu Canyon Road, Malibu, California 90265, USA

[c]Materials and Processes Laboratory, General Motors Research and Development Center, Warren, MI 48090-9055, USA

*Corresponding author email: frederick.e.pinkerton@gm.com

Abstract: Enhanced kinetic performance and reversibility have been achieved with uncatalyzed $NaAlH_4$ by incorporation into nanoporous carbon aerogel. Aerogel with a pore size distribution peaked at 13 nm and a pore volume of 0.8 cm^3/g was filled with $NaAlH_4$ to 94% capacity by melt-infusion at 189 °C under 183 bar H_2 gas overpressure. Dehydrogenation to NaH + Al with reasonable kinetics was accomplished at 150 °C, well below the $NaAlH_4$ melting temperature (183 °C), compared to hydrogen release above 230 °C for bulk uncatalyzed $NaAlH_4$. Uncatalyzed bulk samples did not rehydrogenate under laboratory conditions, whereas $NaAlH_4$ in a carbon aerogel host was readily rehydrogenated at ~160 °C and 100 bar H_2 to ~85% of its initial capacity. Ball-milled $NaAlH_4$ catalyzed with 4 mol% $TiCl_3$ showed somewhat better kinetics compared to the infused aerogel; nevertheless, the large kinetic enhancement obtained by incorporation into carbon aerogel, even in the absence of a catalyst, demonstrates the substantial benefit of confining the $NaAlH_4$ to nanoscale dimensions.

PACS numbers: 62.23.St; 68.43.Nr; 82.20.-w; 82.33.Ln; 84.60.Ve

Introduction

Complex hydrides are of considerable scientific and technological interest as hydrogen storage materials in large part because they offer high volumetric densities of hydrogen (50-115 g hydrogen/liter),[1] substantially larger than that obtainable with high pressure compressed H_2 gas (36.7 g H_2/liter at 700 bar). Sodium alanate ($NaAlH_4$) has been one of the most extensively studied of the complex hydrides.[2-7] It reversibly releases hydrogen in two separate steps:

$$NaAlH_4 \leftrightarrow 1/3\ Na_3AlH_6 + 2/3\ Al + H_2 \quad (1a)$$

$$\leftrightarrow NaH + Al + 3/2\ H_2 \quad (1b)$$

with theoretical hydrogen releases of 3.7 and 1.9 wt%, respectively, totaling 5.6 wt% (70 g H_2/liter). The two steps are characterized by enthalpies of hydrogen release ΔH_d = 37 kJ/mol H_2 (with corresponding equilibrium temperature T(1 bar) ~ 30 °C) for $NaAlH_4$ and 47 kJ/mol H_2 (T(1 bar) = 100 °C) for Na_3AlH_6. While these hydrogen release reactions are thermodynamically allowed at relatively low temperatures compared to many other complex hydrides, the fact that hydrogen release is accompanied by phase separation limits the kinetic performance of these materials. Hydrogen release and reabsorption require bulk diffusion not only of hydrogen but also of the metallic elements in order to accomplish phase separation and recombination. In fact, uncatalyzed bulk $NaAlH_4$ generally does not release hydrogen until reaching temperatures above melting (T_m = 183 °C), and is very difficult to reverse, i.e., does not readily reabsorb hydrogen under laboratory H_2 pressures and temperatures.[2,8] A decade ago Bogdanović et al. discovered that doping $NaAlH_4$ with titanium, accompanied by nanoscale fabrication (for example by ball-milling), reduced the dehydrogenation temperature to below melting and improved the kinetics of dehydrogenation and rehydrogenation to practical values.[2]

More recently it has been reported that kinetic performance can be enhanced by incorporating metal hydrides into a nanoporous matrix.[9-14] Particle sizes, and hence

diffusion distances, are limited by the nanoscale dimensions of the pores, while the pore walls prevent sintering and grain growth during hydrogen cycling. Improved hydrogen desorption and absorption kinetics compared to bulk $NaAlH_4$ have been reported for $NaAlH_4$ incorporated into porous carbon matrices with ~10 nm pores (Schüth et al.[10]), 22 nm diameter $NaAlH_4$ particles supported on carbon nanofibers (Baldé et al.[11,12]), and $NaAlH_4$ incorporated into mesoporous silica with 10 nm pores (Zheng et al.[13]). In this work we investigate the effect of confining $NaAlH_4$ in nanoporous carbon aerogel, and similarly find greatly improved kinetic performance and cyclability compared to bulk sodium alanate. Uncatalyzed $NaAlH_4$ melt-infused into the carbon aerogel reversibly cycles hydrogen with kinetic performance approaching that of catalyzed ball-milled material. Because no catalyst is present, the improved kinetics can be directly ascribed to the nanosized $NaAlH_4$ particles that result from confinement in the aerogel.

Experimental Details

Nanoporous carbon aerogels were synthesized using resorcinol-formaldehyde condensation followed by solvent exchange and pyrolysis, as previously described.[14] Aerogels with a peak in the pore size distribution at ~13 nm and a pore volume of 0.8 cm^3/g were synthesized by mixing 25.88 g (235 mmol) resorcinol, 38.68 g of 36.5 wt % formaldehyde solution in water (470 mmol formaldehyde), 15.40 g deionized water, and 0.050 g (0.472 mmol) sodium carbonate. The solution was transferred to polypropylene jars, sealed, and aged 24 hrs at room temperature, followed by 24 hrs at 50 ºC, and finally another 72 hrs at 90 ºC. The samples were then cooled, cut into rectilinear pieces, and immersed in acetone to displace water. The acetone bath was poured off and refilled twice with a soak time of at least one hour after the first two cycles and 8 hours after the third cycle. The aerogel pieces were dried in air and then heated in a tube furnace under nitrogen from room temperature to 800 °C at 2.6 °C/min and maintained at 800 °C for 6 hours to pyrolyze the resorcinol-formaldehyde gel. Pore size distribution, surface area, and pore volumes were characterized with N_2 absorption at Micromeritics Analytical Services (Norcross, GA) using Brunner-Emmett-Teller (BET) and Barrett-Joyner-Halenda (BJH) analysis.[15] Pieces of aerogel were prepared for infusion by drying at 400

°C under vacuum for at least one hour, then transferring the aerogel into a glove box without air exposure.

Experiments conducted at HRL used $NaAlH_4$ purchased from Aldrich and purified by dissolving the as-received gray powder in dried tetrahydrofuran (THF), removing the insoluble contaminants by centrifugation, and recovering the pure $NaAlH_4$ by evaporating the solvent. At GM the $NaAlH_4$ powder was purchased from Albermarle and used without purification after analyses via X-ray diffraction (XRD) and thermogravimetric analysis (TGA) indicated no significant contaminants. Melt infusion was performed in a PARR pressure vessel rated at 3000 psi. A piece of aerogel together with a stoichiometric quantity of $NaAlH_4$ just sufficient to fill the pore volume of the aerogel was placed into a quartz tube within the vessel. Loading was performed in a glove box to protect against atmospheric contamination. The vessel was sealed and removed from the glove box, evacuated, and filled with H_2 gas to 1700 psig (118 bar). The sealed vessel was then heated to 189 °C, reaching a pressure of 183 bar, and held for 8-10 hr. At these temperatures and H_2 pressures, $NaAlH_4$ melted without decomposition[3] and the aerogel pores filled with molten alanate via capillary action. Measurements of aerogel mass before and after melt-infusion indicate that the sample was 48.6 wt% $NaAlH_4$ and that the aerogel pore volume was filled to 94% capacity with $NaAlH_4$.

For purposes of comparison, a sample of $NaAlH_4$ catalyzed by $TiCl_3$ was made by ball-milling purified $NaAlH_4$ with 4 mol% $TiCl_3$ for 1 hr at 400 RPM in a Fritsch P6 mill. An additional $NaAlH_4$-graphite control sample was made using 1-2 μm synthetic graphite (Aldrich) that had been dried at 400 °C in vacuum. The $NaAlH_4$ and graphite were combined in about the same weight ratio as the $NaAlH_4$-aerogel sample by hand mixing in a mortar and pestle until uniform in color. The effect of ball-milling alone was evaluated by ball-milling pure $NaAlH_4$ without catalyst in a high-energy SPEX 8000 mixer/mill for 5 hrs. Unprocessed $NaAlH_4$ served as the final control sample.

Hydrogen desorption into flowing Ar gas was measured by thermogravimetric analysis (TGA) using a TA Instruments 2950 analyzer (HRL) or a Perkin-Elmer System

7 TGA (GM). Hydrogen cycling experiments were performed at HRL using a custom, stainless steel volumetric gas sorption (Sieverts) apparatus, as described elsewhere.[16] Scanning electron microscope (SEM) images were acquired on a Hitachi S-4800 SEM. X-ray diffraction (XRD) patterns were obtained on samples sealed in glass capillary tubes using a Philips PW3040/60 X'Pert Pro diffractometer (HRL) or a Bruker General Area Detector Diffraction System (GADDS) (GM). Temperature dependent *in situ* XRD was also performed using the GADDS system, as previously described.[17] The XRD samples were loaded under Ar into 1.0 mm diameter quartz capillary tubes and mounted within a custom built furnace. Attachment to a pressure manifold ensured that the evolved hydrogen gas could bleed away from the sample during heating at 1 °C/min.

Results and Discussion

The pore size distribution of the carbon aerogel is illustrated in Fig. 1. The distribution peaks at about 13 nm, with a total pore volume of 0.8 cm^3/g and a micropore-to-mesopore volume ratio of about 0.18:1.[14] An SEM image of the aerogel, shown in Fig. 2, confirms an open porous structure consistent with an average pore size near 13 nm.

TGA weight loss curves for uncatalyzed bulk $NaAlH_4$, uncatalyzed ball-milled $NaAlH_4$, uncatalyzed $NaAlH_4$ infused into carbon aerogel ($NaAlH_4$@aerogel), and ball-milled $NaAlH_4$ + 4 mol% $TiCl_3$ are compared in Fig. 3. The $NaAlH_4$@aerogel, uncatalyzed bulk $NaAlH_4$, and uncatalyzed ball-milled $NaAlH_4$ were heated at 5 °C/min, and an additional scan at 1 °C/min is included for the $NaAlH_4$@aerogel sample. The catalyzed $NaAlH_4$ sample was heated at 3 °C/min. Previous experience indicates that heating at 3 °C/min rather than 5 °C/min shifted the curve toward lower temperature by about 10 °C compared to scanning at 5 °C/min, thus the effects of different heating rates are not significant compared to the large temperature differences between samples. Uncatalyzed bulk $NaAlH_4$ released a small amount of hydrogen as it melted, but then released most of its hydrogen only at temperatures above about 230 °C. The instabilities near 250 °C arise from foaming of the melt during desorption. As is evident from the

knee at 285 °C, desorption occurred in two steps of 3.7 and 1.8 wt%, in excellent correspondence with the two desorption steps in Reaction (1). Continued weight loss above 300 °C is attributed to decomposition of NaH and volatilization of Na. Ball-milling uncatalyzed $NaAlH_4$ for 5 hrs produced no significant kinetic difference from bulk $NaAlH_4$; evidently even such vigorous milling did not change the particle morphology compared to bulk powder sufficiently to favor low temperature desorption. The catalyzed $NaAlH_4$ + 4 mol% $TiCl_3$ sample showed the expected large kinetic improvement for dehydrogenation, with first and second step onsets of ~85 and ~135 °C, respectively. The reduced quantity of hydrogen desorbed is consistent with the 10% mass dilution of $NaAlH_4$ by the $TiCl_3$. Finally, we observe that the dehydrogenation kinetics of uncatalyzed $NaAlH_4$@aerogel was also dramatically superior to that of both bulk and ball-milled uncatalyzed $NaAlH_4$. Although not as low in temperature as the catalyzed $NaAlH_4$ sample, the dehydrogenation onset of ~140 °C nevertheless clearly demonstrates that incorporation of $NaAlH_4$ into nanoporous aerogel substantially improved its kinetic performance even in the absence of a catalyst, and reduced the onset of dehydrogenation to a temperature substantially below the melting temperature. The reduced capacity reflects dilution by the aerogel mass; the 2.4 wt% total weight loss to 250 °C agrees reasonably well with the predicted loss of 2.7 wt% based on the estimated weight fraction of $NaAlH_4$ in the aerogel.

The cycling behaviors of three different $NaAlH_4$-based samples are shown in Fig. 4, along with the temperature profiles used for dehydrogenation into initial vacuum (upper panel) and rehydrogenation using 100 bar initial H_2 pressure (lower panel). For ease of comparison, the wt% reported for all samples has been corrected for the fraction of $NaAlH_4$ in the sample, so that hydrogen desorption and absorption values are relative to the $NaAlH_4$ component. All samples were initially in the hydrogenated state, so each cycle began with dehydrogenation (upper panel). Curves (a) represent the behavior of a control sample consisting of uncatalyzed $NaAlH_4$ + graphite in about the same weight ratio as in the $NaAlH_4$@aerogel sample. As expected for bulk uncatalyzed $NaAlH_4$, dehydrogenation of $NaAlH_4$+graphite occurred only above the melting temperature of $NaAlH_4$, and with poor kinetics even at 200 °C. The $NaAlH_4$ + graphite control sample

also showed no significant reversibility (lower panel). The control sample demonstrates that the kinetic improvements for $NaAlH_4$@aerogel do not rely on the presence of carbon, i.e., the carbon has no catalytic effect.

The best kinetic performance was obtained with $TiCl_3$-catalyzed $NaAlH_4$ (curves b), as shown for two and one-half cycles in Fig. 4. There was a significant reduction in dehydrogenation kinetics between the initial (b1) and second (b2) cycles, after which the cycling appeared stable. $NaAlH_4$@aerogel (curves c), although not quite as good, was both reversible, even though there is no catalyst present, and had kinetic performance that approached that of cycled $TiCl_3$-catalyzed $NaAlH_4$. The $NaAlH_4$@aerogel cycled twice to nearly full capacity, although a minor loss of capacity during the initial cycle was suggested. The first and second rehydrogenations are virtually identical (lower panel, (c)), however, suggesting that the capacity was stable after the first dehydrogenation.

Samples of $NaAlH_4$@aerogel were produced both at HRL and at GM by comparable techniques. As a check of reproducibility, Fig. 5 shows TGA results from two $NaAlH_4$@aerogel samples, one synthesized and measured at HRL and the other melt-infused and measured at GM under comparable conditions using aerogel made at HRL. Good agreement was obtained for the two independent samples and measurements, showing that the synthesis procedure was robust. The small difference in quantity desorbed most likely reflects slightly different $NaAlH_4$ loadings. Comparison of the dehydrogenation rates dW/dt confirmed that the rates and peak temperatures were comparable between the two samples. While the measured peak temperatures are slightly above the equilibrium melting temperature of $NaAlH_4$, the first desorption step (1a) was already complete and the $NaAlH_4$ was totally depleted before this temperature was reached, thus no melting occurred. The concurrence between the two samples demonstrates that $NaAlH_4$ experienced a similar nanoscale environment in the two infused aerogel samples.

One notable feature of the TGA curves for $NaAlH_4$@aerogel in both Fig. 3 and Fig. 5 is that dehydrogenation appeared to occur in a single step rather than two resolved

steps as in bulk $NaAlH_4$ either with or without catalyst. In order to verify the decomposition path, *in situ* XRD was performed on an $NaAlH_4$@aerogel sample. The temperature dependence of the phase composition is summarized in Fig. 6. Each phase present in the sample is represented by the integrated intensity of one characteristic XRD peak: $NaAlH_4$ (112), Na_3AlH_6 (220), Al (111) and NaH (111). The small intensity observed for NaH below 165 °C was due to a slight interference from the $NaAlH_4$ (112) peak. Fig. 7 shows full XRD patterns at three selected temperatures (120 °C, 166 °C, and 195 °C) from among the 274 patterns collected in the course of the temperature-dependent in situ experiment, illustrating important stages in the phase evolution of the sample. At 120 °C the sample consists of $NaAlH_4$ with a small amount of Al; at 166 °C the sample has transformed according to Reaction 1(a) into Na_3AlH_6 and Al; and at 195 °C the sample has converted according to Reaction 1(b) into NaH and additional Al. Even though a single step was observed in the TGA, the *in situ* XRD unambiguously showed that it actually consisted of two nearly commensurate steps characterized by the formation and then disappearance of Na_3AlH_6, consistent with Reactions (1a, 1b), and ending in the products NaH and Al. The 1 °C/min heating rate should be slow enough to accentuate subtle details in the transformations; nevertheless the Al signature changes smoothly with temperature, as does the corresponding TGA curve in Fig. 3. Evidently nanoscale confinement improved the second stage (Reaction (1b)) kinetics more than that of Reaction (1a), which nearly eliminated the 25-30 °C onset delay of Reaction (1b) observed here in the uncatalyzed bulk $NaAlH_4$ and the $TiCl_3$-catalyzed $NaAlH_4$, as well as in other $NaAlH_4$ materials as previously reported.[17] The first dehydrogenation step (1a) then became the rate-limiting step in the dehydrogenation kinetics of $NaAlH_4$@aerogel.

Observation of kinetic enhancement even without a catalyst suggests combining nanoscale confinement with use of a catalyst to explore the possibility of synergistic effects. Work is in progress to attempt to co-infuse $NaAlH_4$ and a catalyst into carbon aerogel.

Conclusion

We have successfully incorporated pure $NaAlH_4$ into 13 nm carbon aerogel by infusion of the melt at 189 °C under 183 bar H_2 gas pressure. The $NaAlH_4$ melt filled the aerogel pores to 94% capacity by capillary action. $NaAlH_4$@aerogel displayed a greatly reduced dehydrogenation temperature, with an onset at ~140 °C, compared to both bulk $NaAlH_4$ and extensively ball-milled $NaAlH_4$ (> 230 °C). Unlike uncatalyzed bulk sodium alanate, $NaAlH_4$@aerogel was readily rehydrogenated to full capacity at ~160 °C under 100 bar H_2. Although the first dehydrogenation of catalyzed bulk $NaAlH_4$ was superior to that of $NaAlH_4$@aerogel, the dehydrogenation kinetics of $NaAlH_4$@aerogel rivaled that of catalyzed bulk $NaAlH_4$ after the first cycle. No enhancement was observed for $NaAlH_4$ mixed with graphite, clearly demonstrating that the presence of carbon alone was insufficient for improved kinetics. Rather, the confinement of $NaAlH_4$ to nanoscale dimensions within aerogel pores, which both limited diffusion distances for phase segregation and recombination and blocked agglomeration into larger particles with cycling, was responsible for the dramatic improvement of cycling kinetics even in the absence of a catalyst.

Acknowledgements:

The authors would like to thank Robert E. Doty for collection of SEM images, Richard Speer, Jr. for XRD analysis, and Martin Meyer for technical support.

References

1. Herbst J F and Pinkerton F E, “Hydrogen Storage Materials,” in J. Weil, D. Blumel, S. Malmoli, and J. Netting, eds., *McGraw-Hill Yearbook of Science and Technology 2008* (McGraw-Hill, New York, 2008), pp. 172-175
2. Bogdanović B and Schwickardi M 1997 *J. Alloys Compd.* **253-254** 1
3. Bogdanović B, Brand R A, Marjanovic A, SchwickardiM and Tölle J 2000 *J. Alloys Compd.* **302** 36
4. Jensen C M and Gross K 2001 *J. Appl. Phys. A* **72** 213
5. Sandrock G, Gross K and Thomas G 2002 *J. Alloys Compd.* **339** 299
6. Schüth F, Bogdanović B and Felderhoff M 2004 *Chem. Commun.* 2249
7. Bogdanović B, Eberle U, Felderhoff M and Schüth F 2007 *Scripta Mater.* **56** 813
8. Meisner G P, Tibbetts G G, Pinkerton F E, Olk C H and Balogh M P 2002 *J. Alloys Compd.* **337** 254
9. Gutowska A, Li L, Shin Y, Wang C M, Li X S, Linehan J C, Smith R S, Kay B D, Schmid B, Shaw W, Gutowski M and Autrey T 2005 *Angew. Chem. Int. Ed.* **44** 3578
10. Schüth F, Bogdanović B and Taguchi A 2003 patent application WO2005014469
11. Baldé C P, Hereijgers B P C, Bitter J H and de Jong K P 2006 *Angew. Chem. Int. Ed.* **45** 3501
12. Baldé C P, Hereijgers B P C, Bitter J H and de Jong K P 2008 *J. Am. Chem. Soc.* **130** 6761
13. Zheng S, Fang F, Zhou G, Ouyang L, Zhu M and Sun D 2008 *Chem. Mater.* **20** 3954
14. Gross A F, Vajo J J, van Atta S L and Olson G L 2008 *J. Phys Chem. C* **112** 5651
15. Lowell S, Shields J E, Thomas M A and Thommes M 2006 *Characterization of Porous Solids and Powders: Surface Area, Pore Size and Density* (Dordrecht, The Netherlands: Springer)
16. Vajo J J, Mertens F, Ahn C C, Bowman Jr R C and Fultz B J 2004 *Phys. Chem. B* **108** 13977
17. Balogh M P, Tibbetts G G, Pinkerton F E, Meisner G P, and Olk C H 2003 *J. Alloys Compd.* **350** 136

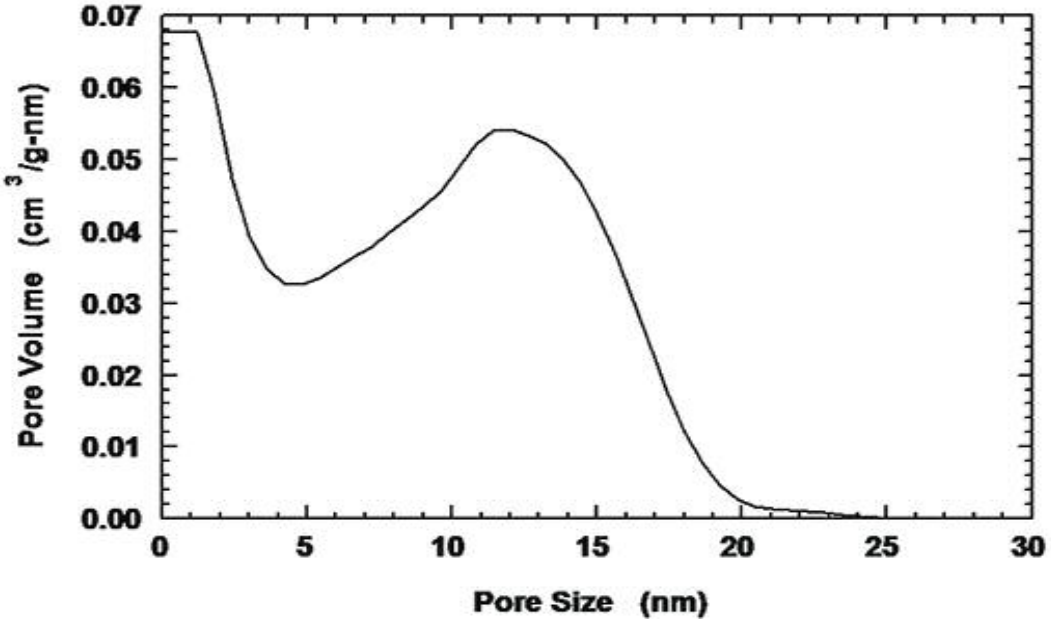

Figure 1. Pore size distribution of the carbon aerogel used in these experiments derived from an N_2 absorption isotherm.

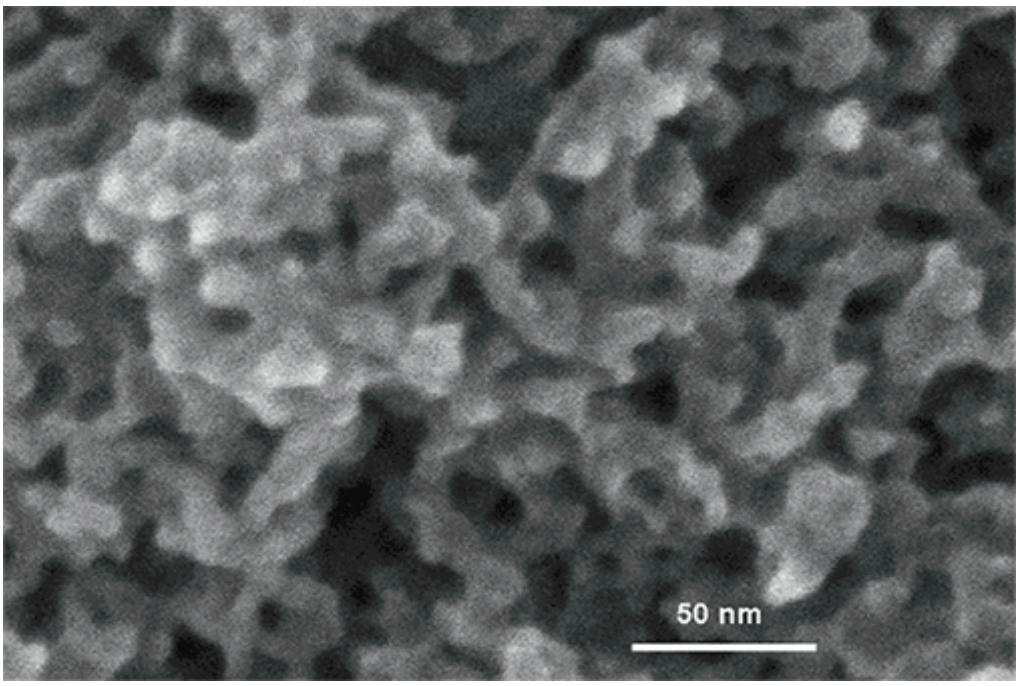

Figure 2. SEM image of the pore structure of 13 nm carbon aerogel.

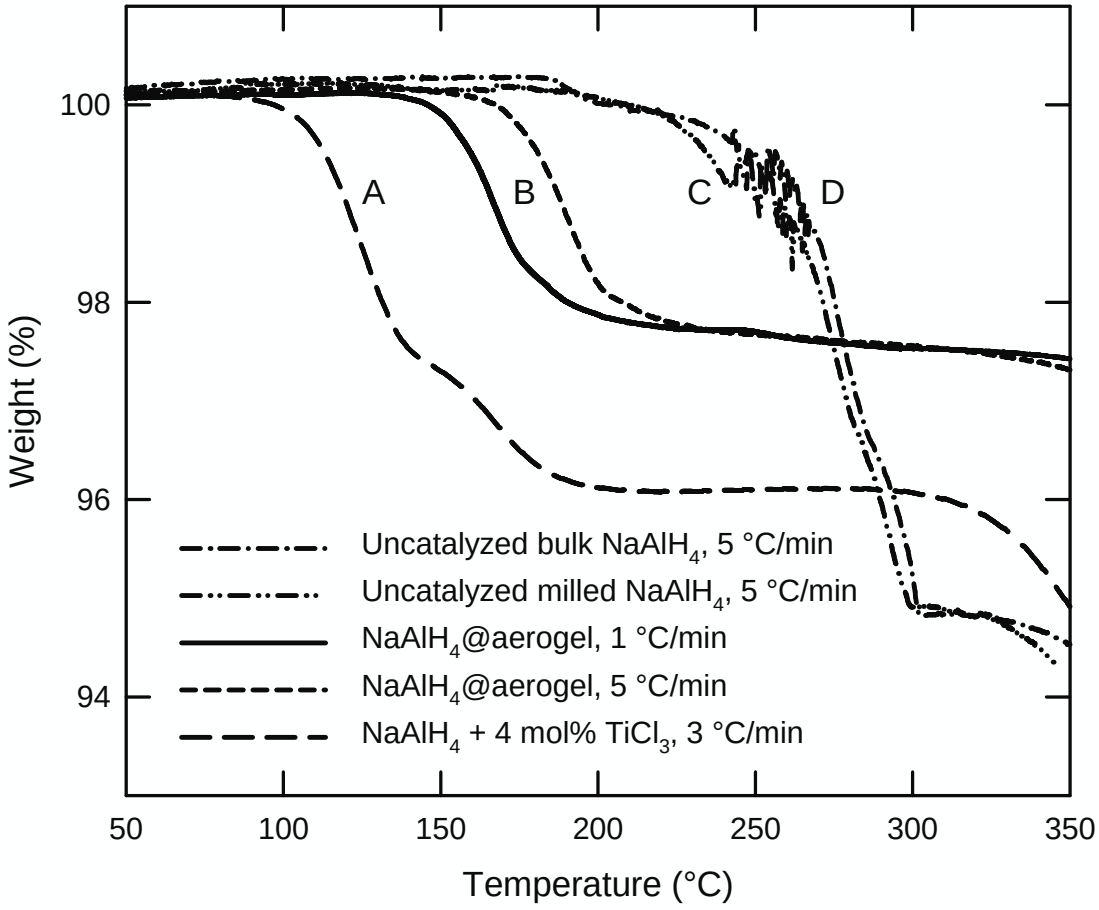

Figure 3. Thermogravimetric analysis (TGA) of four $NaAlH_4$ materials: A) ball-milled $NaAlH_4$ catalyzed with 4 mol% $TiCl_3$, B) uncatalyzed $NaAlH_4$ melt-infused into 13 nm aerogel, C) uncatalyzed $NaAlH_4$ ball-milled for 5 hrs, and D) bulk uncatalyzed $NaAlH_4$. The heating rates are specified in the legend. The $NaAlH_4$ content of the catalyzed sample is 90 wt%, while $NaAlH_4$@aerogel is 48.6 wt% $NaAlH_4$.

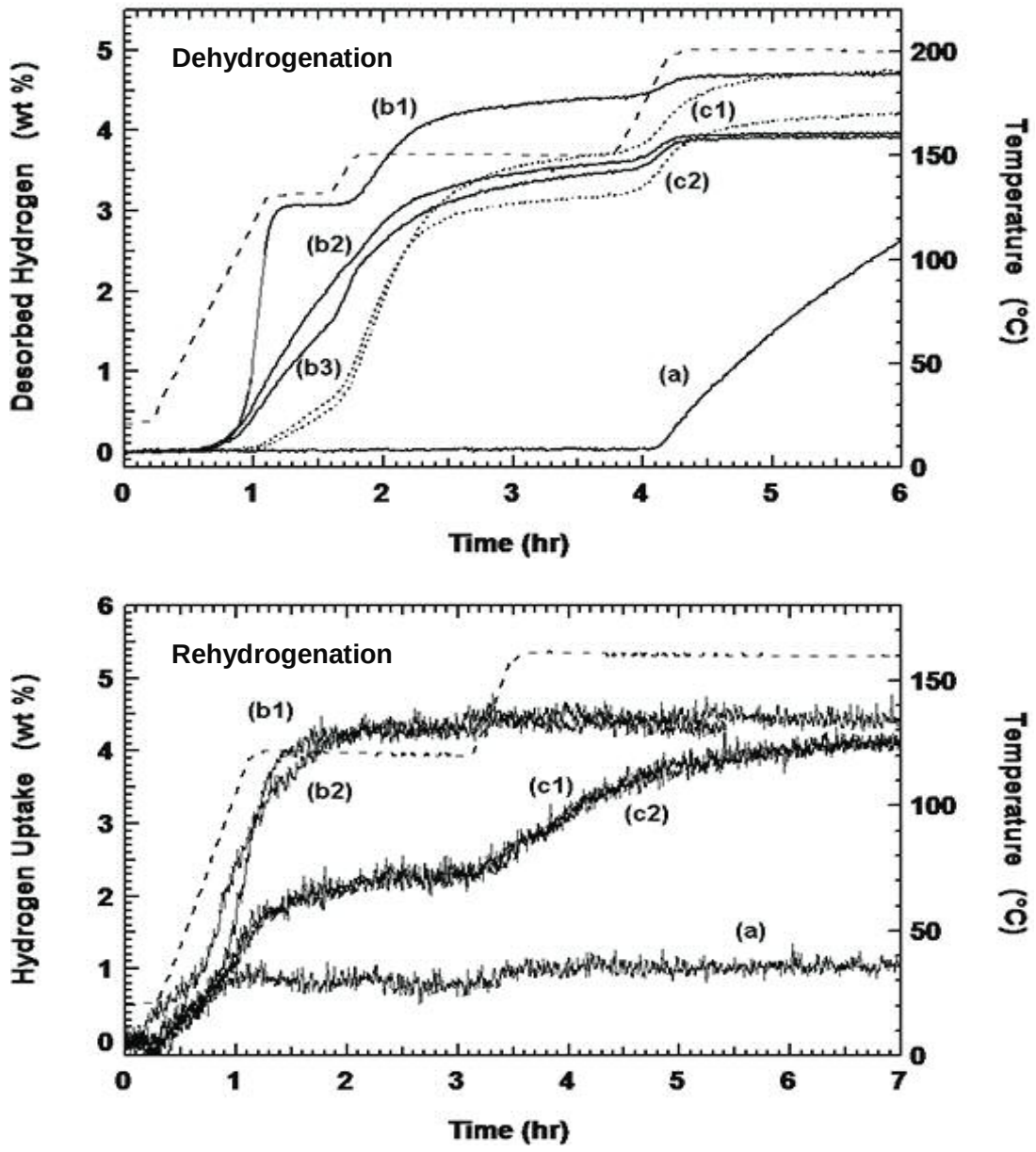

Figure 4. Cycling behavior of $NaAlH_4$: (a) uncatalyzed $NaAlH_4$ mixed with graphite, (b) $TiCl_3$-catalyzed $NaAlH_4$, and (c) $NaAlH_4$ melt-infused into 13 nm carbon aerogel. The numbers indicate the cycle number, where appropriate. The upper panel shows hydrogen evolution during dehydrogenation, and the lower panel shows hydrogen uptake during rehydrogenation. All samples began in the hydrogenated state. The temperature profiles are indicated by the dashed lines.

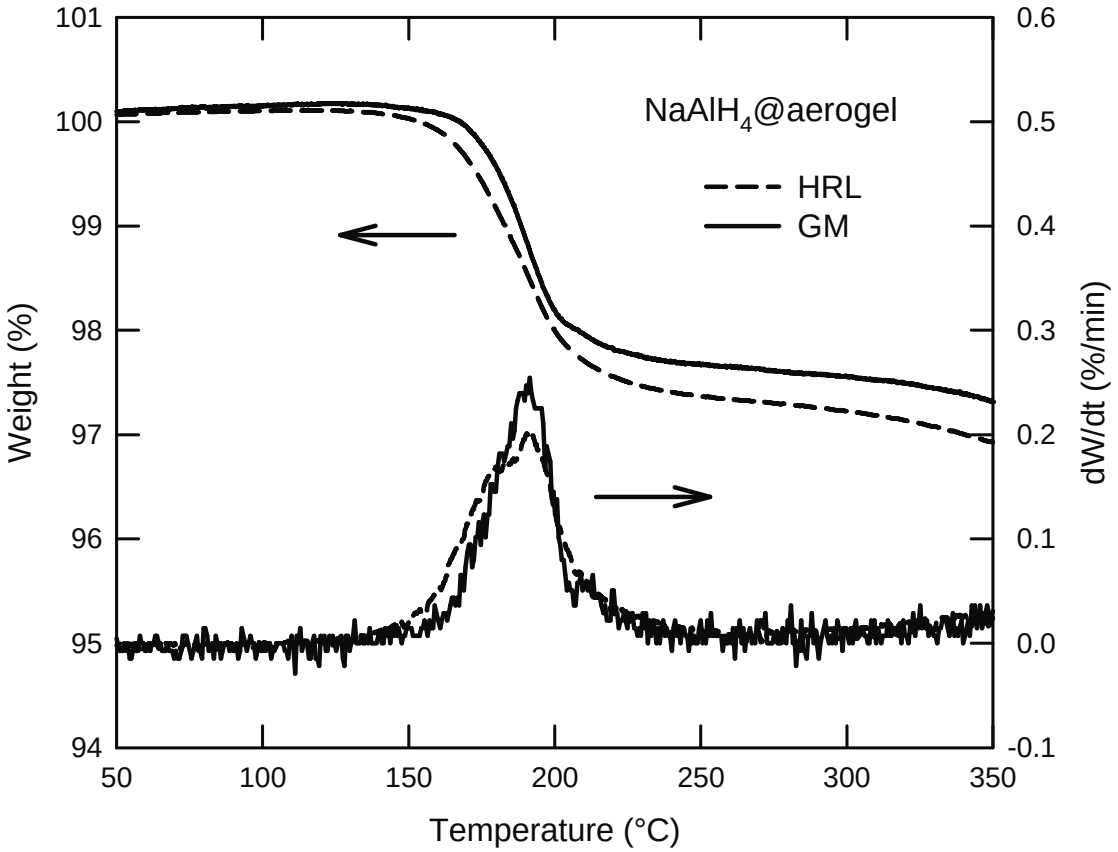

Figure 5. Thermogravimetric analysis (TGA) of the weight loss for two $NaAlH_4$@aerogel samples, one synthesized and measured at HRL and one at GM. Also shown is the first derivative of the weight loss showing the temperature at which the maximum rate of weight loss occurs.

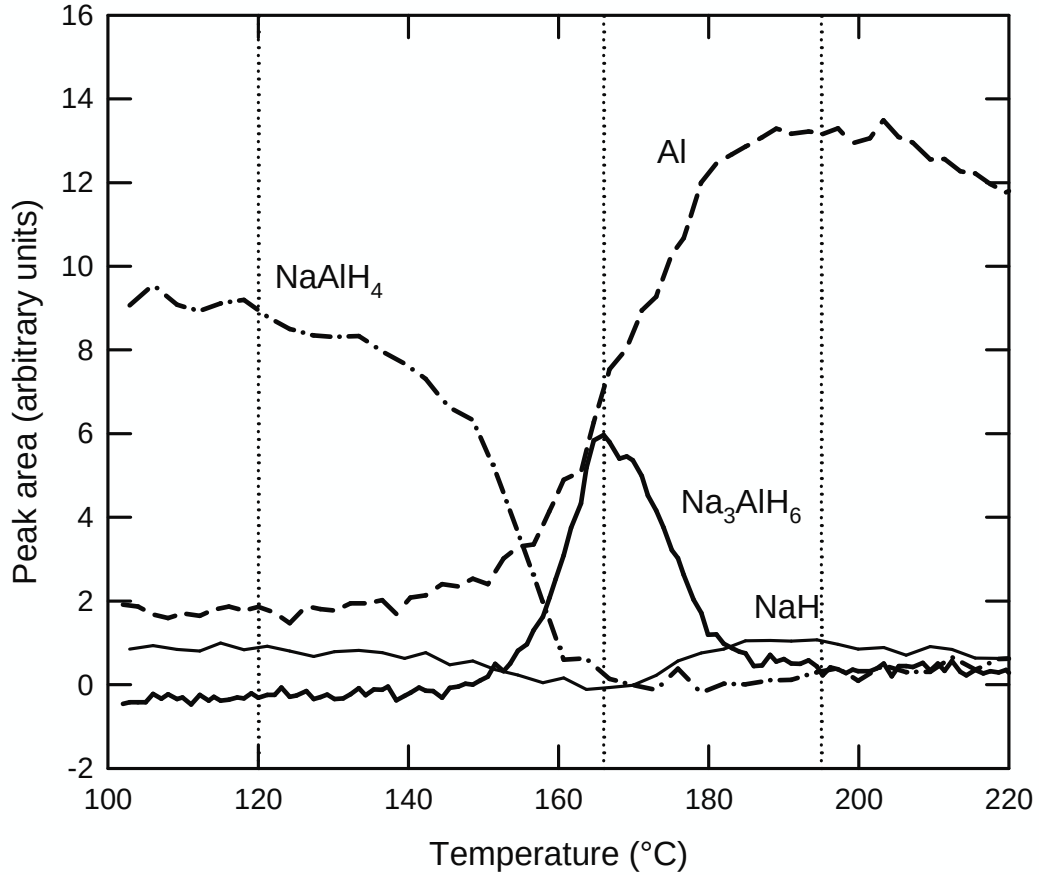

Figure 6. *In situ* XRD of $NaAlH_4$@aerogel heated at 1 °C/min. Shown is the temperature evolution of the integrated intensity under a characteristic diffraction peak of $NaAlH_4$ (112), Na_3AlH_6 (220), Al (111), and NaH (111). The data indicate that both Reactions 1a and 1b occur in the aerogel even though they are not distinct in the TGA data. The intensity observed for NaH below 165 °C is due to a slight interference from an $NaAlH_4$ peak. Vertical dotted lines indicate the temperatures corresponding to the full XRD spectra shown in Fig. 7.

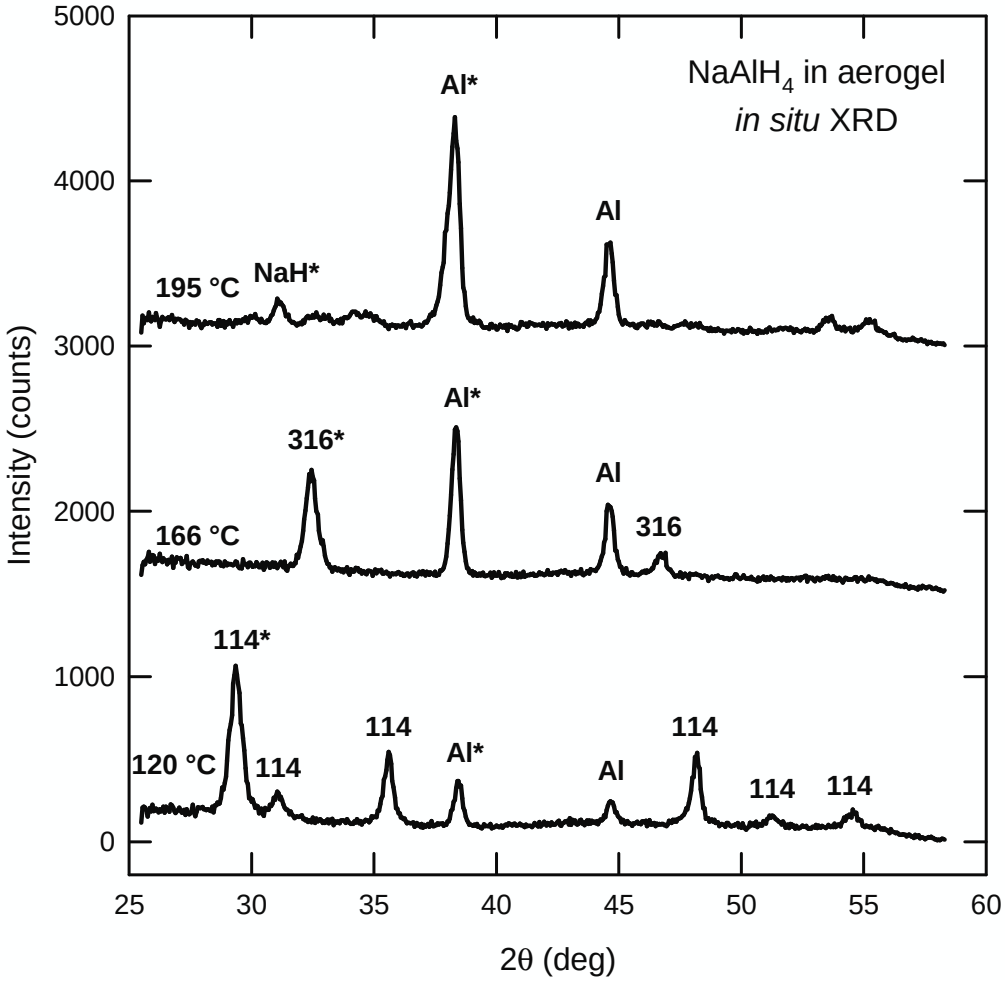

Figure 7. Full XRD patterns from in situ XRD of $NaAlH_4$@aerogel at three selected temperatures. Peaks labeled "114" are indexed as belonging to $NaAlH_4$, and those labeled "316" are from Na_3AlH_6. Peaks indicated with an asterisk (*) are those used to generate the temperature dependence of peak area displayed in Fig. 6. These patterns demonstrate the evolution of phase composition through two transformations from $NaAlH_4$ (with a small amount of excess Al), through Na_3AlH_6 + Al, to NaH with additional Al. Patterns at intermediate temperatures are a superposition of those shown. The XRD pattern at 195 °C also contains two unidentified peaks near 55 deg.